Supporting Information

An efficient synthetic method for cage-like energetic frameworks with high-energy density and appropriate oxygen balance.

Yunzhi Liu [a], Jinyuan Wang [a], Zhenxin Yi [a], Qi Zhou [a], Tianjiao Hou [b], Guixiang Wang [a], Yu Zhang [a,*], Jun Luo [a,*]

[a] *School of Chemistry and Chemical Engineering, Nanjing University of Science and Technology, Nanjing 210094, China.*
[b] *College of Chemical Engineering, Nanjing Tech University, Nanjing 211816, China*

Table of contents

1. Experimental sections

1.1 Caution!

Although we have encountered no accident during preparation and handling of compounds described in this paper, they are potentially explosive energetic materials which are sensitive to impact and friction. Any manipulations must be carried out by using appropriate standard safety precautions. Operators must be equipped with safety equipment such as gloves coats, face shield and explosion-proof baffle.

1.2 Materials and reagents

1,3,5,7-cyclooctatetraene was supplied by Sigma-Aldrich. Unless otherwise specified, the chemicals (AR grade) were obtained from commercial sources and were used without further purification.

1.3 Characterization methods

^{1}H and ^{13}C NMR spectra were recorded on Bruker DPX- 500 instrument at 500 and 126 MHz, respectively, using $CDCl_3$, methanol-d_4, DMSO-d_6 and acetone-d_6 as the solvent with TMS as the internal standard. All IR spectra were obtained by Thermo Nicolet iS10 spectrometer equipped with a Thermo Scientific Smart iTR diamond ATR accessory. TGA and DSC were measured with TGA/SDTA851e and DSC823e, respectively, at a scan rate of 5 °C·min^{-1}. Density of compound **5** was determined at 25 °C by employing a Micromeritics AccuPyc II 1340 gas pycnometer. Impact and friction sensitivity measurements are made by using a standard BAM Fall hammer and a BAM friction tester. Single-crystal X-ray diffraction measurements were conducted on a Bruker D8 CMOS detector employing graphite-monochromated Mo-Kα radiation (λ=0.71073 Å) and Cu-Kα radiation (λ=1.54178). The known compounds were identified by comparison of their physical and spectral data with those reported in the literature. Yields refers to isolated yield of analytically pure material unless otherwise noted.

1.4 Synthesis

tetraepoxide 7

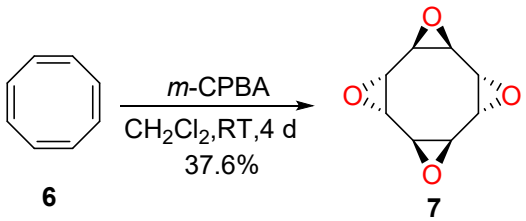

6 **7**

To a suspension of *m*-CPBA (1.0 g, 5 mmol, 85%) in 5 mL of CH_2Cl_2 at 0 °C was added dropwise a solution of compound **6** (52.1 mg, 0.5 mmol) in 20 mL of CH_2Cl_2. After being stirred at room temperature for 4 days, the solution was diluted with an additional 30 mL of CH_2Cl_2, washed with 10% aqueous $NaHSO_3$ (10 mL), 5% $NaHCO_3$ (30 mL), H_2O (30 mL), and then dried over Na_2SO_4 and concentrated in vacuum. The product was purified by flash chromatography (ethyl

acetate/petroleum = 1:150) to afford the tetraepoxide **7** (31.6 mg, 37.6%) as a colorless crystalline solid. ^{1}H NMR (500 MHz, chloroform-*d*) δ 3.18 (s, 1H). ^{13}C NMR (126 MHz, chloroform-*d*) δ 52.74.

2,6-dinitro-2,6-diazaadmantane-4,8,9,10-tetrayl tetranitrate (1) and 2,6-dinitro-2,6-diazahomonoradmantane-4,8,9,10-tetrayl tetranitrate (2)

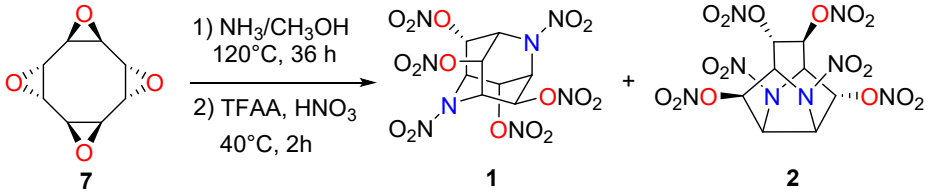

To a solution of **7** (31.6 mg, 0.19 mmol) in 5 mL of CH_3OH was added 10 mL of ammonia-saturated CH_3OH. The mixture was heated to 120 °C for 36 h in a steel bomb. After cooling, the mixture was concentrated in vacuum to afford the crude product (36.5 mg). To a mixture of trifluoroacetic anhydride (3 mL) and 98% fuming nitric acid (2 mL) at 0 °C was added the above crude product. The reaction mixture was heated to 40 °C. After stirring for 2 h, the reaction mixture was cooled to ambient temperature and poured into ice-water (20 mL) with agitation. The white participate was filtered, washed with water and dried in vacuum. The product was purified by flash chromatography (1:150 ethyl acetate/petroleum) to afford compound **1** (11.4 mg, 12.7% over 2 steps) as a white solid, along with compound **2** (26.2 mg, 29.2% over 2 steps) as a white solid, too.

Compound **1**: ^{1}H NMR (500 MHz, acetone-d_6) δ 5.99 (d, J = 3.9 Hz, 1H), 5.96 (d, J = 2.5 Hz, 1H). ^{13}C NMR (126 MHz, acetone-d_6) δ 71.51, 51.88. IR (thin film, υ/cm^{-1}): 2917, 2846, 1650, 1535, 1276, 1104, 811, 795, 734, 651. Elemental analysis calcd (%) for $C_8H_8N_8O_{16}$: C 20.35, H 1.71, N 23.73; found: C 20.37, H 1.72, N 23.70.

Compound **2**: ^{1}H NMR (500 MHz, acetone-d_6) δ 6.19 (d, J = 6.8 Hz, 1H), 6.06 (s, 1H), 5.98 (s, 1H), 5.93 (d, J = 6.8 Hz, 1H). ^{13}C NMR (126 MHz, acetone-d_6) δ 80.17, 77.08, 65.70, 61.74. IR (thin film, υ/cm^{-1}): 2928, 2358, 1656, 1541, 1276, 1098, 1066, 816, 739. Elemental analysis calcd (%) for $C_8H_8N_8O_{16}$: C 20.35, H 1.71, N 23.73; found: C 20.36, H 1.73, N 23.71.

3,8,11-trioxatetracyclo[4.4.1.0^{2,4}.0^{7,9}]undecane-5,10-diol

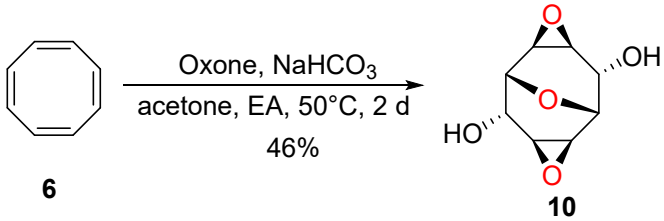

To a 100 mL three-necked flask equipped with dropping funnel and thermometer were added $NaHCO_3$ (0.96g, 11.4mmol), water (10 mL), acetone (1.45 mL, 10mmol), ethyl acetate (20 mL) and **6** (52.1 mg, 0.5 mmol). A solution of Oxone (1.53 g, 5mol) in water (15 mL) was added dropwise over 1 h to the vigorously stirred reaction mixture at the rate to keep mixture temperature below 30

°C. After addition, the mixture was heated to 50 °C. After stirring for 24 h, the reaction mixture was cooled to ambient temperature. A solution of Oxone (1.53 g, 5mol) in water (15 mL) was added to the above system below 30 °C. After addition, the mixture was heated to 50 °C for another 24 h, and then quenched by 10% aqueous $NaHSO_3$ (20 mL). Aqueous phase was extracted with ethyl acetate (3 × 30 mL). The combined organic phase was washed with water (20 mL), saturated solution of $NaHCO_3$ (20 mL) and brine (20 mL), dried (Na_2SO_4) and concentrated in vacuum. The product was purified by flash chromatography (ethyl acetate/petroleum = 1:1) to afford compound **10** (42.8 mg, 46%) as a white solid. ^{1}H NMR (500 MHz, methanol-d_4) δ 3.99 (d, J = 8.0 Hz, 4H), 3.43 (d, J = 3.9 Hz, 2H), 3.21 (d, J = 3.9 Hz, 2H). ^{13}C NMR (126 MHz, methanol-d_4) δ 66.29, 63.26, 54.76, 48.22. IR (thin film, υ/cm^{-1}): 3365, 2934, 1712, 1154, 1015, 844, 573. Elemental analysis calcd (%) for $C_8H_{10}O_5$: C 51.61, H 5.41; found: C 51.63, H 5.42.

6-nitro-2-oxa-6-azaadamantane-4,8,9,10-tetrayl tetranitrate (3), 2-nitro-7-oxa-2-azaprotoamantane-4,5,9,10-tetrayl tetranitrate (4), 7-nitro-2-oxa-7-azatwistane 4,5,9,10-tetrayl tetranitrate (5)

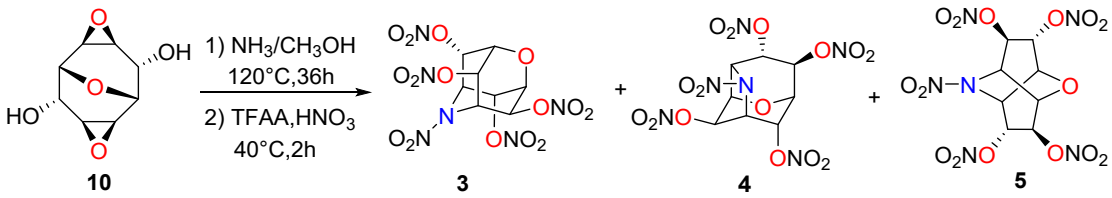

To a solution of compound **8** (42.8 mg, 0.23 mmol) in 5 mL of CH_3OH was added 10 mL of ammonia-saturated CH_3OH. The mixture was heated to 120 °C for 24 h in a steel bomb. After cooling, the mixture was concentrated in vacuum to afford the crude product (49 mg). To a mixture of trifluoroacetic anhydride (3 mL) and 98% fuming nitric acid (2 mL) at 0 °C was added the above crude product. The reaction mixture was heated to 40 °C. After stirring for 2 h, the reaction mixture was cooled to ambient temperature and poured into ice-water (20 mL) with agitation. The white participate was filtered, washed with water and dried in vacuum. The product was purified by flash chromatography (ethyl acetate/petroleum = 1:100) to afford compound **3** (51.2 mg, 52% over 2 steps) as a white solid, along with compound **4** (11.5 mg, 11.7% over 2 steps) and compound **5** (26.5 mg, 26.9% over 2 steps) as white solids, too.

Compound **3**: ^{1}H NMR (500 MHz, acetone-d_6) δ 5.97 (s, 1H), 5.92 (dd, J = 4.7, 2.3 Hz, 1H), 5.77 (d, J = 4.0 Hz, 1H), 4.82 (d, J = 4.6 Hz, 1H). ^{13}C NMR (126 MHz, acetone-d_6) δ 72.87, 72.48, 66.45, 52.02. IR (thin film, υ/cm^{-1}): 2912, 1648, 1543, 1267, 1029, 819, 787, 731, 674, 457. Elemental analysis calcd (%) for $C_8H_8N_6O_{15}$: C 22.44, H 1.88, N 19.63; found: C 22.45, H 1.90, N 19.61.

Compound **4**: ^{1}H NMR (500 MHz, chloroform-d) δ 5.48 (d, J = 5.6 Hz, 3H), 5.46 (s, 1H), 5.36 (d, J = 5.2 Hz, 1H), 4.82 (d, J = 5.1 Hz, 1H), 4.71 (d, J = 4.0 Hz, 1H), 4.63 (t, J = 4.2 Hz, 1H). ^{13}C NMR (126 MHz, chloroform-d) δ 75.97, 75.94, 74.93, 74.89, 73.52, 73.10, 72.81, 68.94. IR (thin

film, υ/cm^{-1}): 2922, 2352, 1639, 1276, 1025, 834, 750, 677. Elemental analysis calcd (%) for $C_8H_8N_6O_{15}$: C 22.44, H 1.88, N 19.63; found: C 22.47 H 1.91, N 19.60.

Compound **5**: ^{1}H NMR (500 MHz, Chloroform-*d*) δ 5.63 (d, *J* = 3.6 Hz, 1H), 5.59 (dd, *J* = 4.9, 2.2 Hz, 1H), 5.40 (d, *J* = 3.7 Hz, 1H), 4.49 (d, *J* = 4.8 Hz, 1H). ^{13}C NMR (126 MHz, Chloroform-*d*) δ 71.79, 71.23, 66.15, 51.60. IR (thin film, υ/cm^{-1}):2928, 2358, 1656, 1457, 1358, 1098, 1077, 966, 822. Elemental analysis calcd (%) for $C_8H_8N_6O_{15}$: C 22.44, H 1.88, N 19.63; found: C 22.46, H 1.89, N 19.61.

2. Optimization of the reaction conditions for ammonolysis and nitration

In order to explore the optimal reaction conditions for ammonolysis and nitration, we conducted the following experiments using the synthesis of compound **3** as an example.

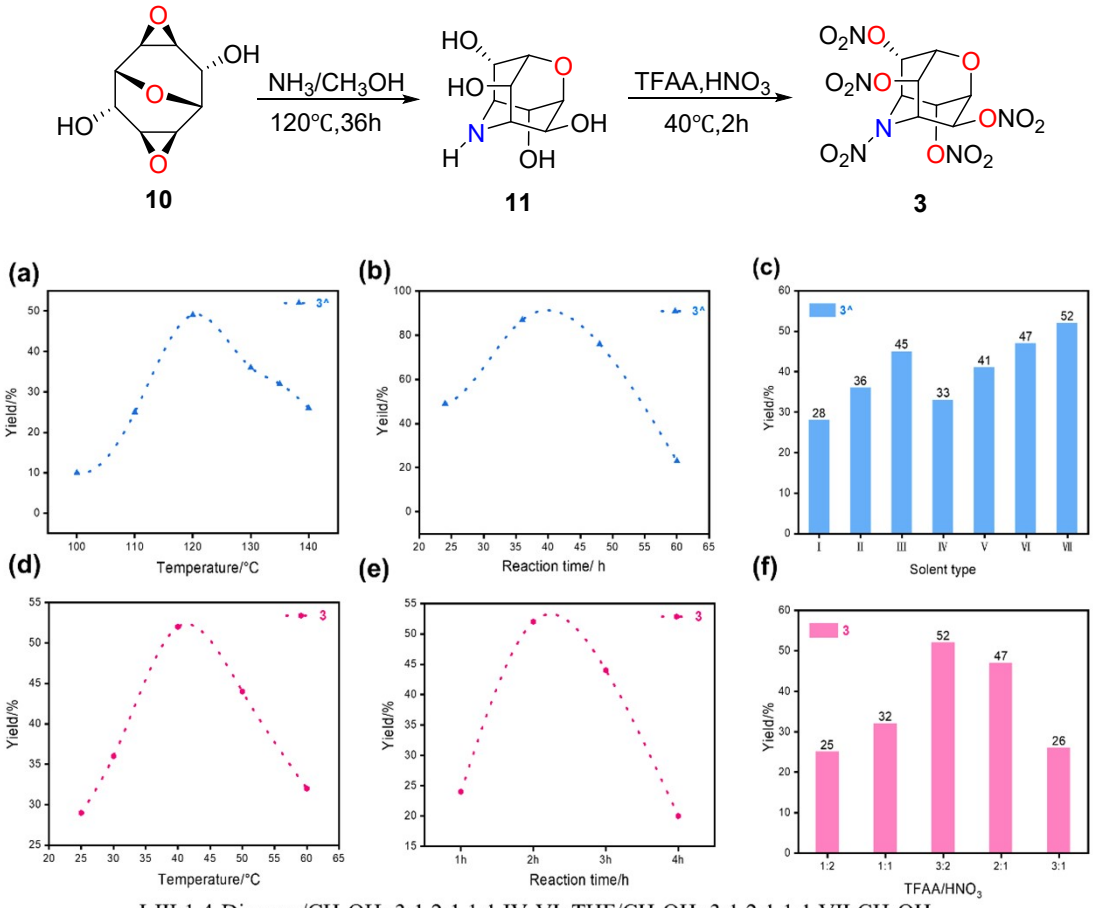

Fig. S1. Influence of reaction temperature (a), reaction time (b), solvent type (c) to intermediate **11**, and reaction temperature (d), reaction time (e), solvent proportion on nitration (f) to **3**.

As illustrated in Fig. S1, when methanol was used as the solvent, in the range of 100~140 °C the yield of compound **11** initially increases but then gradually decreases and the peak values were all found to be at 120 °C. The reason might be attributed to that the reaction was incomplete under relatively low temperature, which was supported by the presence of some residue substrate. While

under too high temperature the dehydration of the products would occur, because dark reaction mixture was resulted and remarkable aromatization by-products might form since the TLC test showed some observable spots under ultraviolet lamp. Thereby, the optimal temperature was determined to be 120 °C. The reaction time affects the reaction dramatically, it can be seen from Fig. S1b that the yield climbed initially and then fell along with the time. The superior reaction time for all the products was determined to be 36 hours. The effect of the reaction solvent on the yield of ammonolysis was demonstrated in Fig. S1c. In THF-MeOH mixed solvents, the yield of **11** increased along with the elevation of the methanol proportion, the same as 1,4-dioxane and methanol systems. However, the two mixed solvent systems were inferior to single methanol. Overall, the methanol is the best choice. The reaction conditions of nitration were systematically explored. It could be deduced from Fig. S1d-f that the optimal conditions for the nitration was reacting at 40 °C for 2 hours in the nitrating reagent with a ratio of 3:2 (TFAA/HNO_3).

3. Crystallographic data

The absolute structures of compounds **1**~**4** was determined using X-ray diffraction techniques. Single crystals of compounds **2** and **4** were successfully obtained through slow recrystallization from a mixture of ethanol and dichloromethane at 2~8 °C in an icebox. While single crystals of compounds **1** and **3** were obtained by slow recrystallization from two different solvent mixtures at room temperature: one from a mixture of ethanol and chloroform, and the other from a mixture of acetone and chloroform. Unfortunately, the single crystal suitable for X-ray diffraction analysis of compound **5** were not obtained despite a number of solvent systems such as acetone, chloroform, dichloromethane, ethanol, and their mixtures were attempted.

Table S1. Crystal data and structure of **1**-**4**

Identification code	**1**	**2**	**3**	**4**
CCDC	2400806	2400811	2400846	2426709
Empirical formula	$C_8H_8N_8O_{16}$	$C_8H_8N_8O_{16}$	$C_8H_8N_6O_{15}$	$C_8H_8N_6O_{15}$
Formula weight	472.22	472.22	428.2	428.2
Temperature/K	298	293.15	298.15	293
Crystal system	orthorhombic	monoclinic	monoclinic	monoclinic
Space group	$P2_12_12_1$	$P2/c$	$P2_1/n$	$P2_1/n$
a/Å	8.8178(5)	14.9850(14)	7.3775(2)	7.3514(18)
b/Å	12.7488(6)	8.7843(8)	23.9959(6)	24.141(6)
c/Å	29.873(2)	14.7467(13)	8.7037(2)	8.7022(18)
α/°	90	90	90	90
β/°	90	119.47	102.5580(10)	101.928(8)
γ/°	90	90	90	90
Volume/Å^3	1195.25(19)	1689.9(3)	1503.95(7)	1511.0(6)
Z	8	8	4	4
ρ_{calc} g/cm^3	1.868	1.856	1.891	1.882
μ/mm^{-1}	1.661	1.65	1.682	0.186

F(000)	1920	960	872	872
Crystal size/mm^3	0.13×0.12×0.11	0.13×0.12×0.11	0.13×0.12×0.11	0.13×0.12×0.11
Radiation	CuKα (λ = 1.54178)	CuKα (λ = 1.54178)	CuKα (λ = 1.54178)	MoKα (λ = 0.71073)
2θ range for data collection/°	5.916 to 136.796	6.776 to 136.68	7.368 to 136.414	5.074 to 55.034
Index ranges	-10≤h≤10, -12≤k≤15, -34≤l≤36	-18≤h≤18, -10≤k≤10, -17≤l≤17	-8≤h≤8, -28≤k≤25, -10≤l≤10	-9≤h≤9, -31≤k≤30, -11≤l≤11
Reflections collected	23712	20928	12123	24684
Independent reflections	6152 [R_{int}= 0.1197]	3089 [R_{int}= 0.0832]	2730 [R_{int}= 0.0343]	3478 [R_{int}= 0.0796]
Data/restraints/parameters	6152/2/577	3089/468/398	2730/4/262	3478/36/281
Goodness-of-fit on F^2	1.024	1.024	1.071	1.104
Final R indexes [I≥2σ (I)]	R_1=0.0788, wR_2=0.1792	R_1=0.0906, wR_2=0.1976	R_1=0.0635, wR_2=0.1765	R_1=0.0658, wR_2=0.1388
Final R indexes [all data]	R_1=0.1094, wR_2=0.1997	R_1=0.1001, wR_2=0.2013	R_1=0.0686, wR_2=0.1800	R_1=0.1028, wR_2=0.1565
Largest diff. peak/hole /eÅ^{-3}	0.37/-0.35	0.41/-0.34	0.59/-0.66	0.41/-0.24

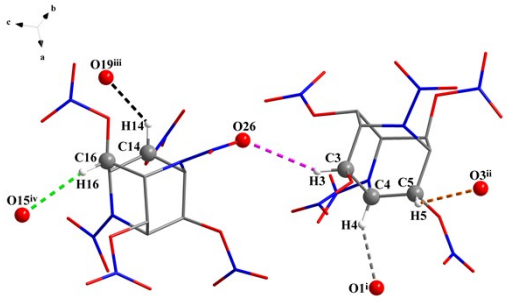

Fig. S2 Hydrogen bond diagram of compound **1**

Table S2. Hydrogen bond table of compound **1**

D-H···A	d(D-H)	d(H···A)	d(D···A)	∠D-H···A
C3-H3···O26	0.98	2.689	3.563	148.83
C4-H4···O1^{i}	0.98	2.471	3.254	136.64
C5-H5···O3^{ii}	0.98	2.57	3.215	123.33
C14-H14···O19^{iii}	0.98	2.425	3.093	125.04
C16-H16···O15^{iv}	0.979	2.476	3.373	152.17

Symmetry codes: i) *x*+1/2, 1/2-*y*, 1-*z*; ii) *x*+1/2, 3/2-*y*, 1-*z*; iii) *x*-1, *y*, *z*; iv) 1-*x*, 1/2-*y*, 3/2-*z*.

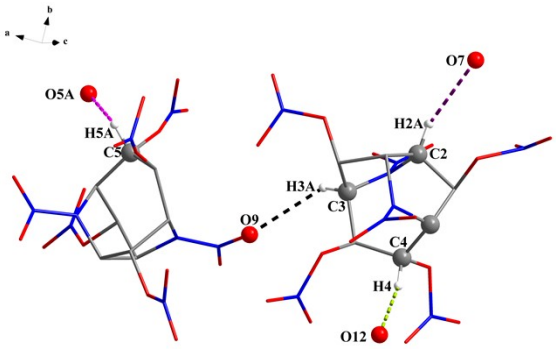

Fig.S3 Hydrogen bond diagram of compound **2**

Table S3. Hydrogen bond table of compound **2**

D-H···A	d(D-H)	d(H···A)	d(D···A)	∠D-H···A
C2-H2B···O7^{i}	0.98	2.713	3.437	131.1
C3-H3A···O9	0.979	2.591	3.266	126.15
C4-H4···O12^{ii}	0.98	2.357	3.294	159.69
C5-H5A···O5A^{iii}	0.98	2.658	3.766	122.64

Symmetry codes: i) -*x*, 1+*y*, 1/2-*z*; ii) -*x*, 1-*y*, -*z*; iii) 1-*x*, 2-*y*, 1-*z*.

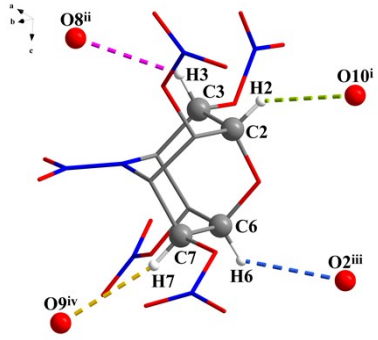

Fig. S4 Hydrogen bond diagram of compound **3**

Table S4. Hydrogen bond table of compound **3**

D-H···A	d(D-H)	d(H···A)	d(D···A)	∠D-H···A
C2-H2···O10^{i}	0.98	2.615	3.408	138.11
C3-H3···O8^{ii}	0.98	2.627	3.402	136.14
C6-H6···O2^{iii}	0.98	2.69	3.342	124.29
C7-H7···O9^{iv}	0.98	2.673	3.626	164.16

Symmetry codes: i) 1-*x*, -*y*, 2-*z*; ii) *x*+1/2, 1/2-*y*, *z*-1/2; iii) 1-*x*, -*y*, 2-*z*; iv) *x*+1/2, 1/2-*y*, *z*+1/2.

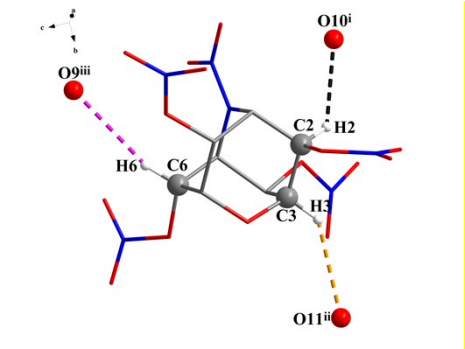

Fig.S5 Hydrogen bond diagram of compound **4**

Table S5. Hydrogen bond table of compound **4**

D-H···A	d(D-H)	d(H···A)	d(D···A)	∠D-H···A
C2-H2···O10i	0.98	2.586	3.372	137.11
C3-H3···O11ii	0.98	2.618	3.412	138.2
C6-H6···O9iii	0.98	2.68	3.629	163.29

Symmetry codes: i) 1/2+*x*, 1/2-*y*, *z*-1/2; ii) 1-*x*, 1-*y*, 1-*z*; iii) 1/2+*x*, 1/2-*y*, 1/2+*z*.

TableS6 Bond Lengths for **1**

Parameter	Length/Å	Parameter	Length/Å
O(1)-N(2)	1.217(11)	O(5)-N(5)	1.404(10)
N(1)-N(2)	1.374(10)	O(5)-C(5)	1.459(9)
N(1)-C(4)	1.482(10)	N(5)-O(6)	1.175(11)
N(1)-C(8)	1.476(10)	N(5)-O(7)	1.233(11)
C(1)-C(2)	1.511(13)	C(5)-C(6)	1.541(11)
C(1)-C(8)	1.541(13)	N(6)-O(8)	1.450(9)
C(1)-O(11)	1.471(11)	N(6)-O(9)	1.204(10)
O(2)-N(2)	1.211(11)	N(6)-O(10)	1.211(11)
C(2)-N(3)	1.463(11)	C(6)-C(7)	1.532(11)
C(2)-C(3)	1.547(12)	N(7)-O(11)	1.425(12)
O(3)-N(4)	1.216(10)	N(7)-O(12)	1.216(13)
N(3)-N(4)	1.418(10)	N(7)-O(13)	1.206(14)
N(3)-C(6)	1.463(10)	C(7)-O(8)	1.461(9)
C(3)-C(4)	1.553(13)	C(7)-C(8)	1.539(11)
C(3)-O(14)	1.442(11)	N(8)-O(14)	1.445(12)
O(4)-N(4)	1.223(10)	N(8)-O(15)	1.196(13)
C(4)-C(5)	1.533(11)	N(8)-O(16)	1.144(14)

TableS7 Bond Angle for **1**

Parameter	Angle/°	Parameter	Angle/°
N(2)-N(1)-C(4)	116.8(7)	O(6)-N(5)-O(7)	130.8(9)
N(2)-N(1)-C(8)	116.7(7)	O(7)-N(5)-O(5)	109.7(9)
C(8)-N(1)-C(4)	116.5(6)	C(4)-C(5)-C(6)	109.5(7)
C(2)-C(1)-C(8)	110.0(8)	O(5)-C(5)-C(4)	106.9(6)
O(11)-C(1)-C(2)	104.3(7)	O(5)-C(5)-C(6)	104.1(6)
O(11)-C(1)-C(8)	109.5(7)	O(9)-N(6)-O(8)	117.7(8)
O(1)-N(2)-N(1)	117.7(9)	O(9)-N(6)-O(10)	132.1(9)
O(2)-N(2)-O(1)	125.1(8)	O(10)-N(6)-O(8)	110.2(9)
O(2)-N(2)-N(1)	117.2(8)	N(3)-C(6)-C(5)	105.3(6)
C(1)-C(2)-C(3)	109.7(7)	N(3)-C(6)-C(7)	110.0(7)
N(3)-C(2)-C(1)	107.3(7)	C(7)-C(6)-C(5)	109.6(6)
N(3)-C(2)-C(3)	107.1(7)	O(12)-N(7)-O(11)	118.8(10)
C(2)-N(3)-C(6)	117.7(6)	O(13)-N(7)-O(11)	110.7(11)
N(4)-N(3)-C(2)	115.8(7)	O(13)-N(7)-O(12)	130.4(12)
N(4)-N(3)-C(6)	115.6(7)	C(6)-C(7)-C(8)	108.9(7)
C(2)-C(3)-C(4)	109.6(7)	O(8)-C(7)-C(6)	110.4(6)
O(14)-C(3)-C(2)	107.1(7)	O(8)-C(7)-C(8)	101.9(6)
O(14)-C(3)-C(4)	107.7(7)	N(6)-O(8)-C(7)	112.7(7)
O(3)-N(4)-N(3)	115.9(8)	O(15)-N(8)-O(14)	109.9(11)
O(3)-N(4)-O(4)	127.4(8)	O(16)-N(8)-O(14)	116.3(10)
O(4)-N(4)-N(3)	116.6(8)	O(16)-N(8)-O(15)	133.5(12)
N(1)-C(4)-C(3)	107.0(7)	N(1)-C(8)-C(1)	109.1(7)
N(1)-C(4)-C(5)	108.9(7)	N(1)-C(8)-C(7)	105.3(7)
C(5)-C(4)-C(3)	107.8(7)	C(7)-C(8)-C(1)	110.5(7)
N(5)-O(5)-C(5)	114.1(7)	N(7)-O(11)-C(1)	115.1(8)
O(6)-N(5)-O(5)	119.5(8)	C(3)-O(14)-N(8)	114.9(8)

TableS8 Bond Lengths for **2**

Parameter	Length/Å	Parameter	Length/Å
O1-N1	1.274(12)	C4-O6	1.428(8)
N1-O2	1.087(11)	N5-N6	1.347(8)
N1-O3	1.298(13)	N5-O9	1.218(7)
C1-C2	1.527(10)	C5-C6	1.566(8)
C1-C3	1.484(10)	N6-C6	1.464(8)
N2A-C22	1.63(4)	N6-C8	1.480(7)
N2A-C3	1.43(2)	N7-O11	1.390(7)
N2-C22	1.469(11)	N7-O12	1.175(9)

N2-N3	1.356(9)	N7-O13	1.168(9)
N2-C3	1.439(9)	C7-C83	1.554(8)
C2-C22	1.527(16)	C7-O11	1.417(7)
C3-C4	1.551(9)	N8-O15	1.187(15)
N4-O6	1.481(9)	N8-O16	1.472(11)
N4-O7	1.175(10)	C8-C83	1.568(12)

Table S9 Bond Angle for **2**

Parameter	Angle/°	Parameter	Angle/°
O1-N1-O3	113.8(8)	O8-N4-O6	110.0(9)
O2-N1-O1	127.2(10)	C41-C4-C3	118.1(4)
O2-N1-O3	118.9(12)	O6-C4-C3	104.9(5)
O3A-C1-C2	91(3)	O9-N5-O10	128.4(7)
O3A-C1-C3	111(5)	O10-N5-N6	116.1(6)
O3-C1-C2	103.8(7)	C6-C5-C52	117.4(4)
O3-C1-C3	112.0(11)	O16-C5-C52	110.0(8)
C3-C1-C2	102.9(5)	O16-C5-C6	104.5(6)
N3A-N2A-C3	122(3)	O16A-C5-C6	112.4(16)
C3-N2A-C21	105(2)	N5-N6-C6	123.1(5)
N3-N2-C21	120.7(7)	N5-N6-C8	120.7(5)
N3-N2-C3	124.1(7)	C6-N6-C8	113.6(5)
C3-N2-C21	112.9(7)	N6-C6-C5	109.5(5)
C1-C2-C21	105.9(8)	C7-C6-C5	114.2(5)
N21-C2-C1	107.0(6)	O12-N7-O11	113.5(8)
N21-C2-C21	101.7(6)	O13-N7-O12	128.5(8)
N1-O3-C1	121.4(9)	O11-C7-C82	104.3(5)
C1-C3-C4	115.2(6)	N6-C8-C72	106.4(5)
N2A-C3-C1	112(2)	N6-C8-C82	102.9(5)
N2A-C3-C4	97(2)	C72-C8-C82	104.1(5)
N2-C3-C1	102.2(6)	N7-O11-C7	115.9(5)
N2-C3-C4	108.0(6)	C5-O16-N8	112.3(7)
O7-N4-O8	129.2(9)	--	

Table S10 Bond Lengths for **3**

Parameter	Length/Å	Parameter	Length/Å
O(1)-N(1)	1.410(3)	N(4)-O(10)	1.412(3)
O(1)-C(1)	1.453(4)	N(4)-O(11)	1.151(4)
N(1)-O(2)	1.182(4)	N(4)-O(12)	1.181(3)

N(1)-O(3)	1.190(4)	C(4)-C(5)	1.526(4)
C(1)-C(2)	1.522(5)	C(4)-N(6)	1.465(4)
C(1)-C(8)	1.531(4)	N(5)-N(6)	1.352(4)
N(2)-O(4)	1.416(4)	N(5)-O(14)	1.218(4)
N(2)-O(5)	1.177(4)	N(5)-O(15)	1.190(4)
N(2)-O(6)	1.128(3)	C(5)-C(6)	1.535(4)
C(2)-C(3)	1.522(4)	C(5)-O(7)	1.439(4)
C(2)-O(13)	1.431(4)	N(6)-C(8)	1.472(4)
N(3)-O(7)	1.422(4)	C(6)-C(7)	1.516(4)
N(3)-O(8)	1.192(5)	C(6)-O(13)	1.436(4)
N(3)-O(9)	1.198(4)	C(7)-C(8)	1.530(4)
C(3)-O(4)	1.441(4)	C(7)-O(10)	1.454(4)
C(3)-C(4)	1.528(4)	-	

Table S11 Bond Angle for **3**

Parameter	Angle/°	Parameter	Angle/°
N(1)-O(1)-C(1)	115.1(2)	N(6)-C(4)-C(3)	105.9(2)
O(2)-N(1)-O(1)	118.6(3)	N(6)-C(4)-C(5)	109.2(2)
O(2)-N(1)-O(3)	129.7(3)	O(14)-N(5)-N(6)	118.0(3)
O(3)-N(1)-O(1)	111.6(3)	O(15)-N(5)-N(6)	117.9(3)
O(1)-C(1)-C(2)	110.9(2)	O(15)-N(5)-O(14)	124.1(3)
O(1)-C(1)-C(8)	104.7(3)	C(4)-C(5)-C(6)	107.9(2)
C(2)-C(1)-C(8)	108.4(2)	O(7)-C(5)-C(4)	110.8(3)
O(5)-N(2)-O(4)	117.2(3)	O(7)-C(5)-C(6)	105.7(2)
O(6)-N(2)-O(4)	114.8(3)	C(4)-N(6)-C(8)	118.0(2)
O(6)-N(2)-O(5)	128.0(4)	N(5)-N(6)-C(4)	120.5(2)
C(1)-C(2)-C(3)	110.3(2)	N(5)-N(6)-C(8)	119.8(2)
O(13)-C(2)-C(1)	108.0(2)	C(7)-C(6)-C(5)	111.3(2)
O(13)-C(2)-C(3)	110.8(2)	O(13)-C(6)-C(5)	108.3(2)
O(8)-N(3)-O(7)	111.9(3)	O(13)-C(6)-C(7)	109.7(2)
O(8)-N(3)-O(9)	130.7(4)	N(3)-O(7)-C(5)	113.6(2)
O(9)-N(3)-O(7)	117.4(3)	C(6)-C(7)-C(8)	108.9(2)
C(2)-C(3)-C(4)	108.9(2)	O(10)-C(7)-C(6)	105.7(2)
O(4)-C(3)-C(2)	109.8(3)	O(10)-C(7)-C(8)	110.2(2)
O(4)-C(3)-C(4)	105.7(2)	N(6)-C(8)-C(1)	108.5(2)
N(2)-O(4)-C(3)	115.7(2)	N(6)-C(8)-C(7)	106.2(2)
O(11)-N(4)-O(10)	118.0(3)	C(7)-C(8)-C(1)	107.7(2)
O(11)-N(4)-O(12)	129.3(3)	N(4)-O(10)-C(7)	114.8(2)

O(12)-N(4)-O(10)	112.6(3)	C(2)-O(13)-C(6)	113.8(2)
C(5)-C(4)-C(3)	108.0(2)	--	

Table S12 Bond Lengths for **4**

Parameter	Length/Å	Parameter	Length/Å
O1-C3	1.433(4)	C3-C4	1.517(5)
O1-C7	1.421(4)	O4-N5	1.181(4)
N1-C1	1.458(4)	N4-O11	1.409(4)
N1-N2	1.361(4)	N4-O12	1.175(4)
N1-C5	1.486(5)	N4-O13	1.182(4)
C1-C8	1.531(4)	O5-N6	1.417(4)
O2-C4	1.447(4)	C5-C6	1.521(6)
O2-N5	1.408(4)	O6-N6	1.160(5)
N2-O14	1.215(4)	N6-O7	1.193(5)
N2-O15	1.204(4)	C6-C7	1.512(5)
C2-C3	1.525(4)	C6-O11	1.480(5)
C2-O5	1.437(4)	C7-C8	1.527(5)
N3-O8	1.428(4)	O8-C8	1.437(4)

Table S13 Bond Angle for **4**

Parameter	Angle/°	Parameter	Angle/°
C7-O1-C3	113.4(2)	N6-O5-C2	114.9(3)
C1-N1-C5	120.2(3)	O3-N5-O2	111.4(3)
N2-N1-C1	121.0(3)	O4-N5-O3	130.0(3)
N1-C1-C2	106.1(3)	N1-C5-C4	109.1(3)
N1-C1-C8	107.9(3)	N1-C5-C6	104.1(3)
C2-C1-C8	108.0(3)	C6-C5-C4	106.2(4)
N5-O2-C4	115.2(3)	O6-N6-O5	118.3(3)
O14-N2-N1	118.3(3)	O6-N6-O7	130.4(4)
O15-N2-N1	116.9(3)	O7-N6-O5	111.3(4)
O15-N2-O14	124.8(3)	C7-C6-C5	109.0(3)
C1-C2-C3	109.3(3)	O11-C6-C5	107.5(3)
O5-C2-C1	105.9(3)	O11-C6-C7	108.3(3)
O5-C2-C3	109.9(3)	O1-C7-C6	109.1(3)
O9-N3-O8	117.5(4)	O1-C7-C8	108.6(2)
O10-N3-O9	130.6(4)	C6-C7-C8	114.3(3)
O1-C3-C4	107.6(3)	N3-O8-C8	113.5(3)
C4-C3-C2	111.3(3)	C7-C8-C1	106.6(3)

O12-N4-O11	112.4(3)	O8-C8-C1	110.3(3)
O12-N4-O13	130.5(3)	O8-C8-C7	105.7(3)
O13-N4-O11	117.1(3)	C4-C6A-O11	127.8(12)
O2-C4-C5	102.6(3)	C5A-C6A-O11	93.0(11)
C3-C4-C5	107.7(3)	N1-C5A-C7	113.5(9)
C6A-C4-O2	125.6(7)	C6A-C5A-N1	100.9(12)
C6A-C4-C3	113.9(7)	C6A-C5A-C7	97.4(12)

4. NMR Spectra of compounds

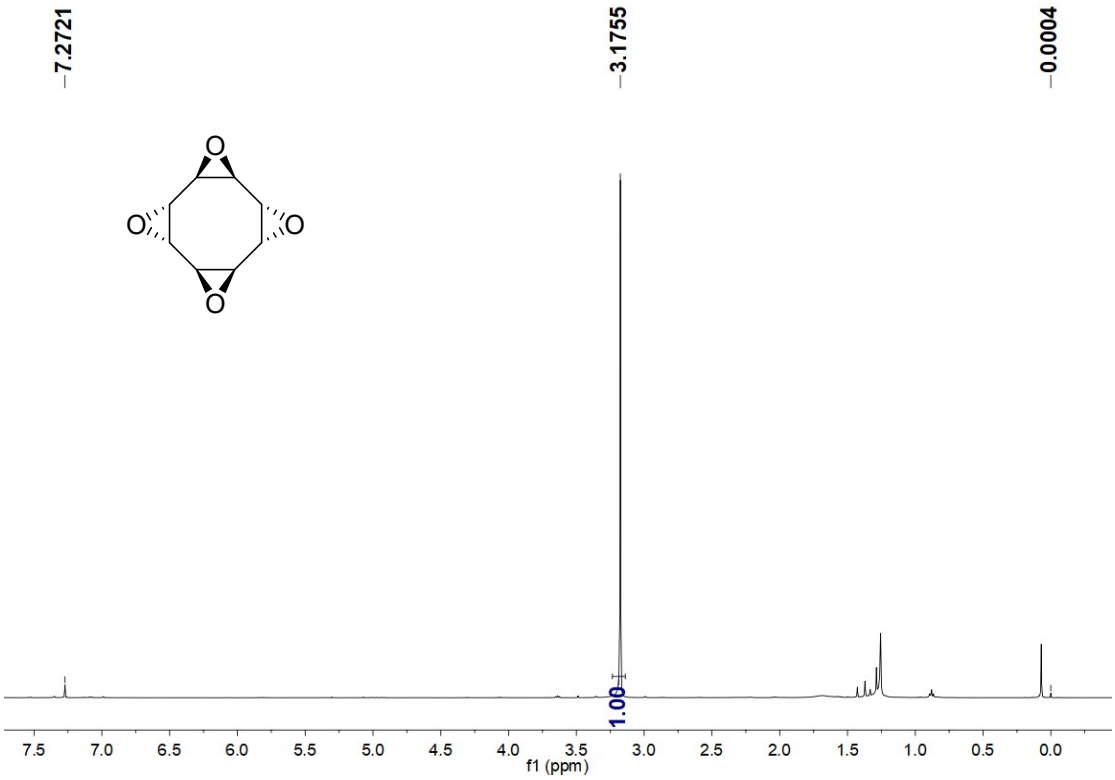

Fig. S6 ^{1}H NMR spectrum of compound **7** ($CDCl_3$, 500 MHz)

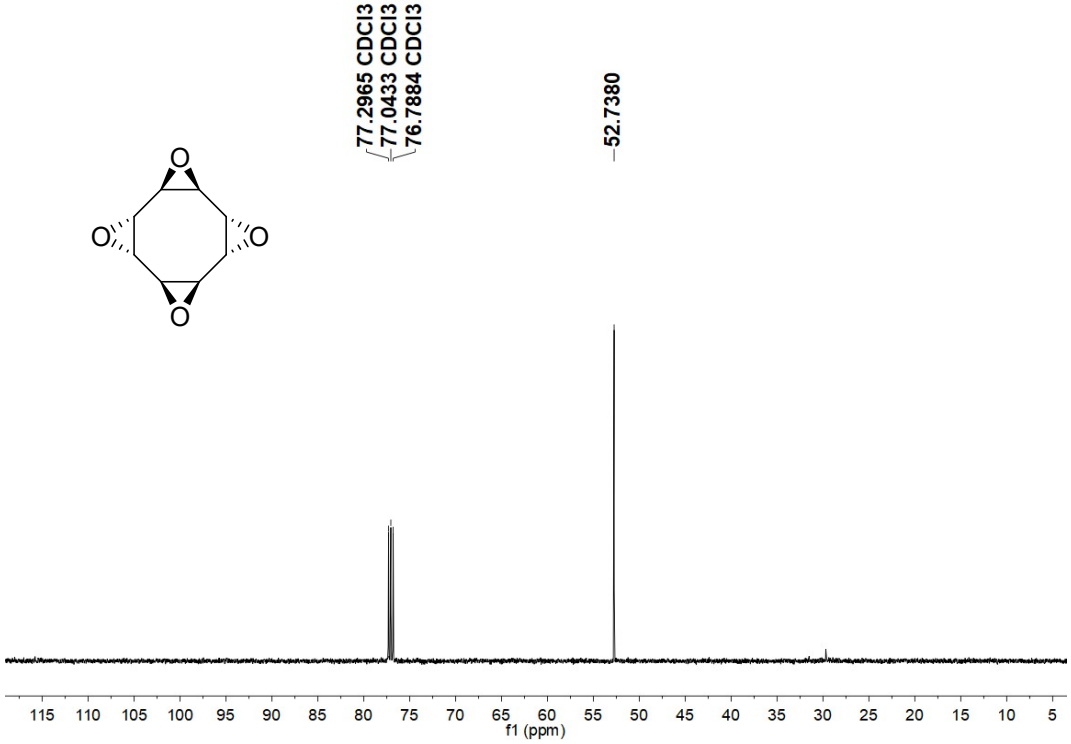

Fig. S7 ^{13}C NMR spectrum of compound **7** ($CDCl_3$, 126 MHz)

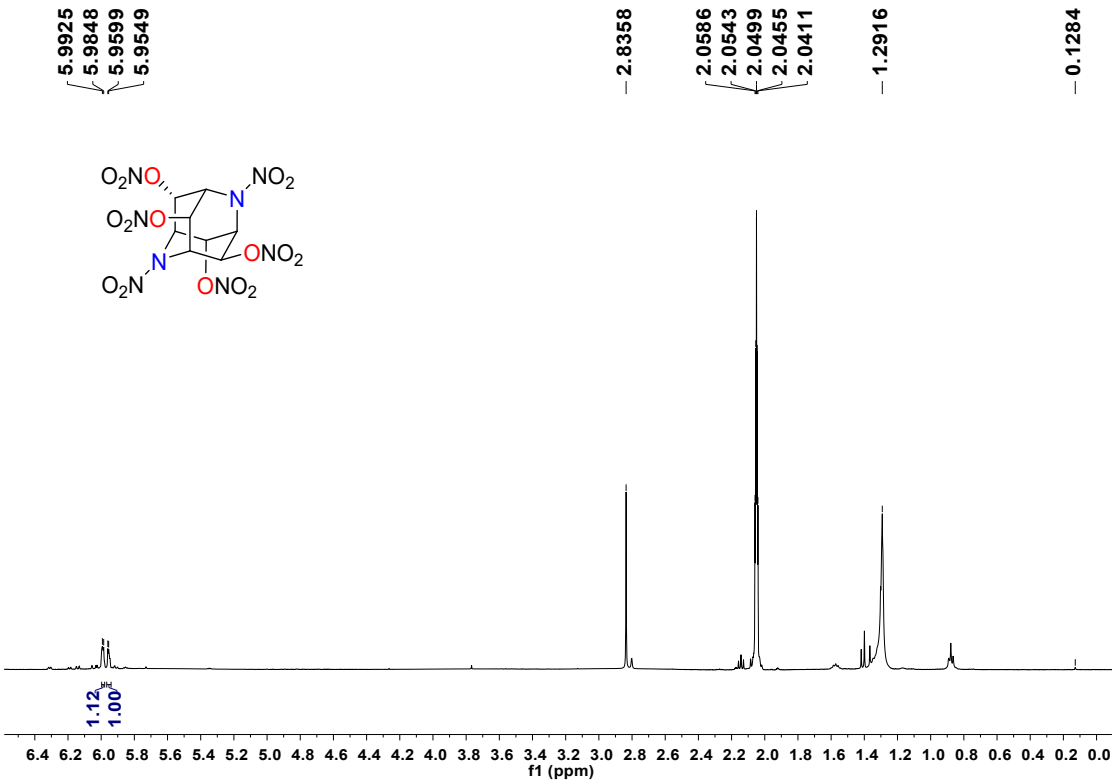

Fig. S8 ^{1}H NMR spectrum of compound **1** (acetone-*d*6, 500 MHz)

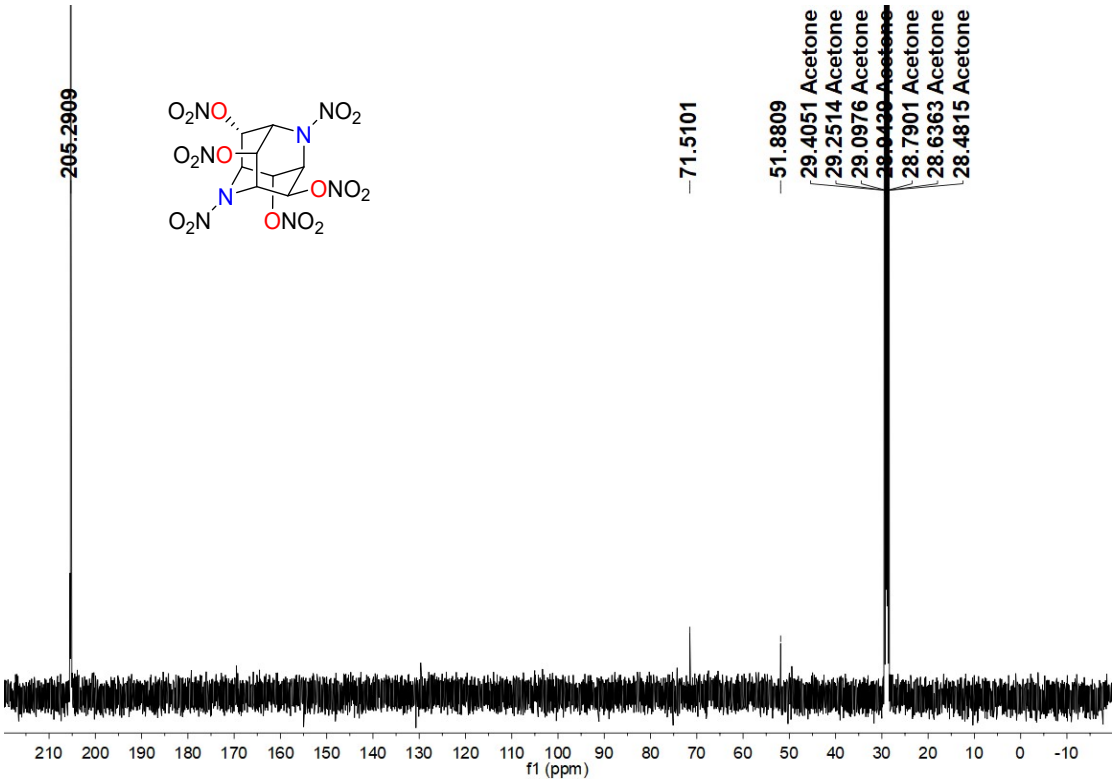

Fig.S9 ^{13}C NMR spectrum of compound **1** (acetone-*d*6, 126 MHz)

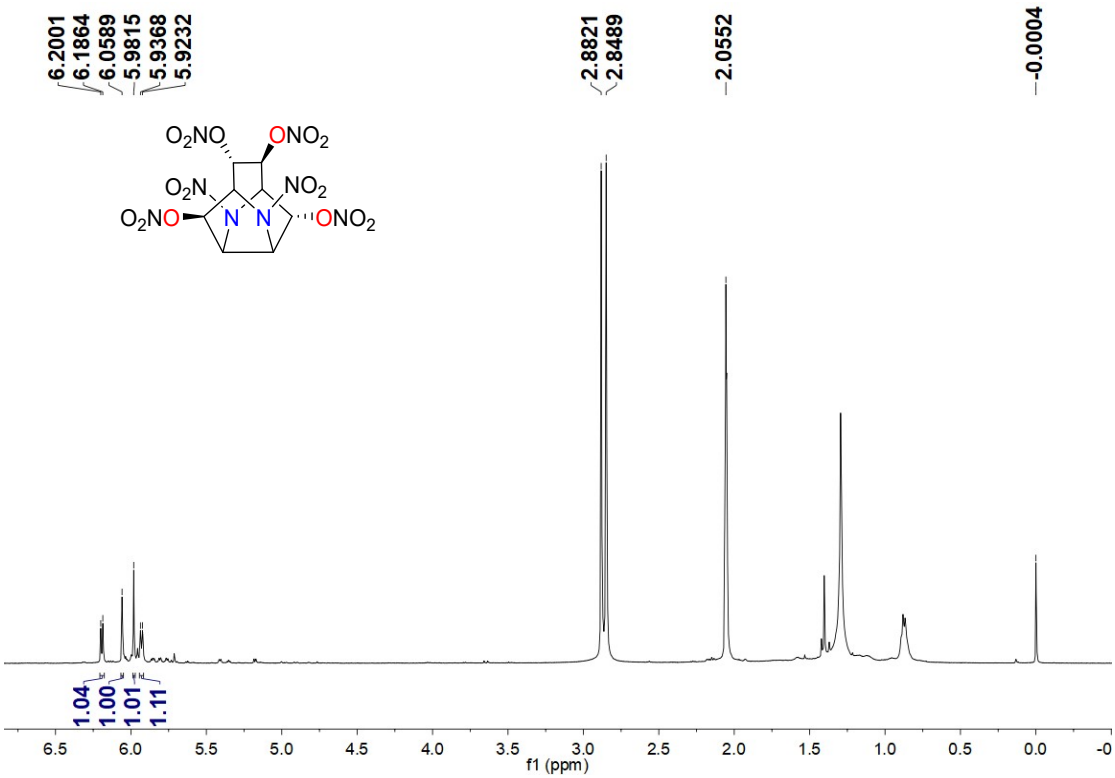

Fig.S10 ^{1}H NMR spectrum of compound **2** (acetone-*d*6, 500 MHz)

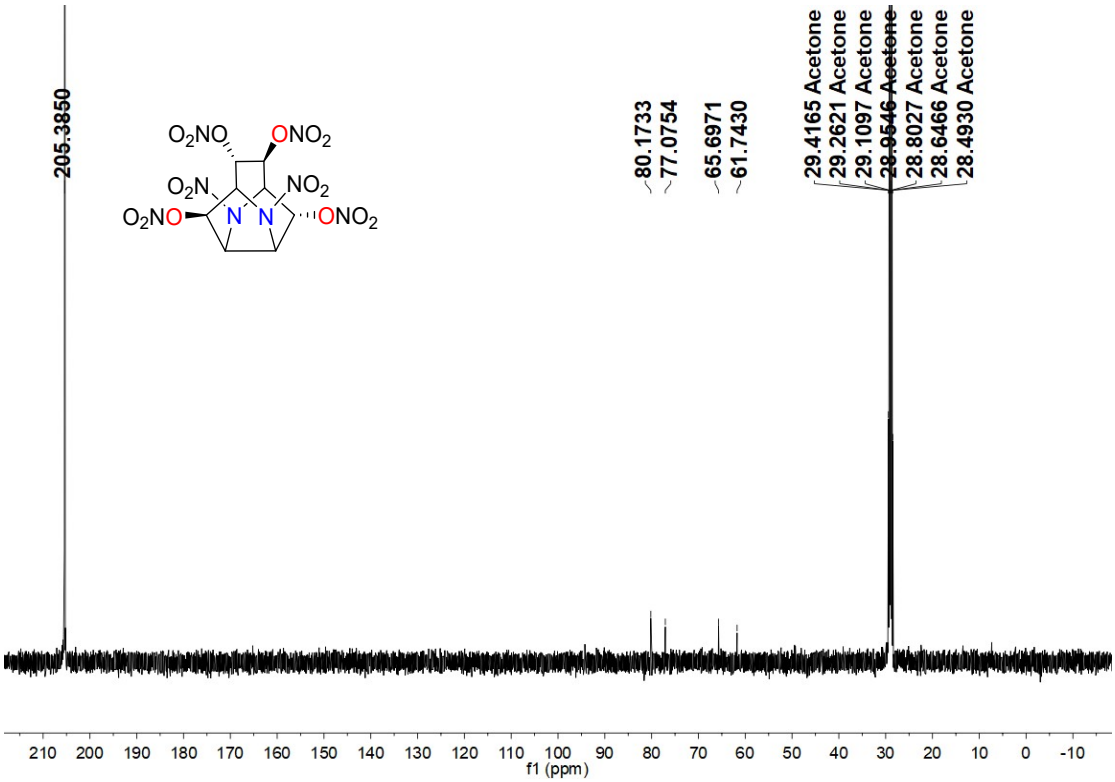

Fig.S11 ^{13}C NMR spectrum of compound **2** (acetone-d_6, 126 MHz)

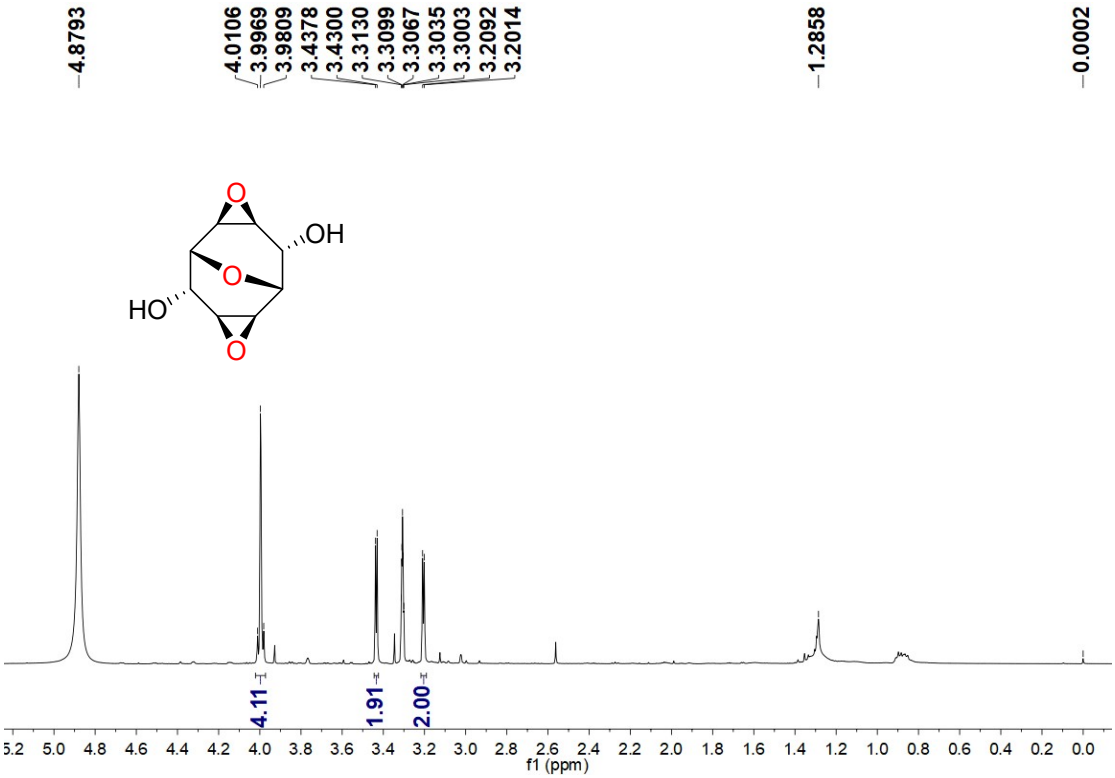

Fig.S12 ^{1}H NMR spectrum of compound **10** (methanol-*d*4, 500 MHz)

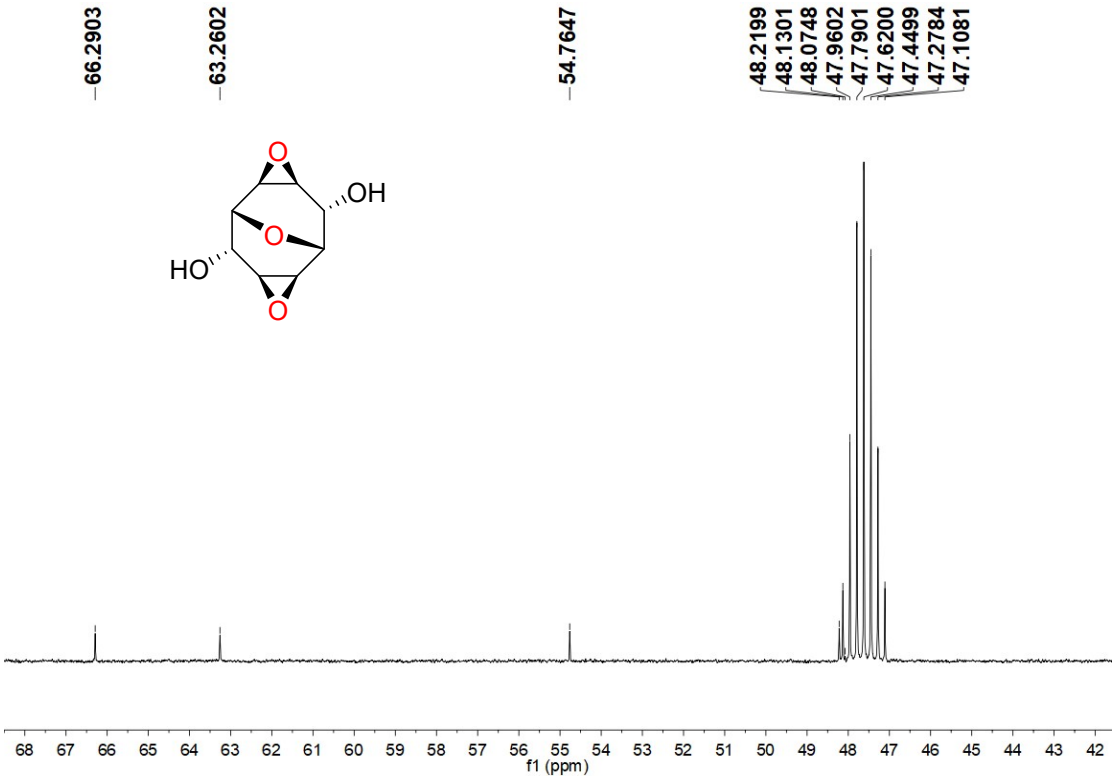

Fig.S13 ^{13}C NMR spectrum of compound **10** (methanol-*d*4, 126 MHz)

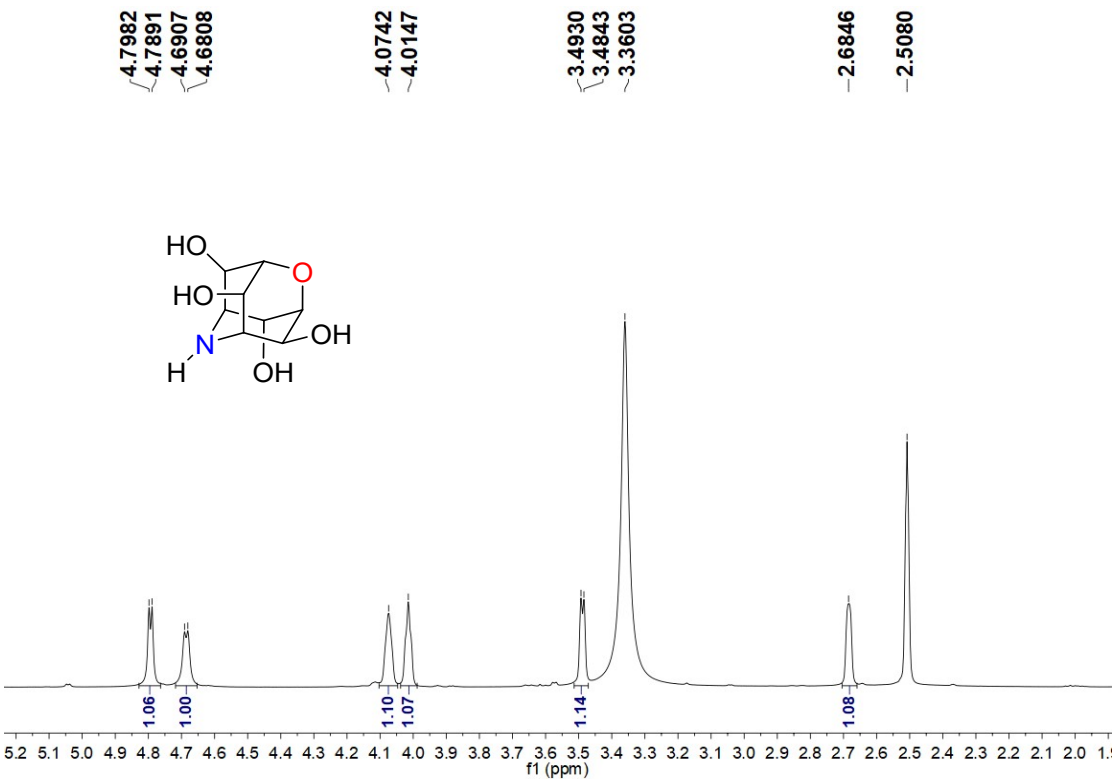

Fig.S14 ^{1}H NMR spectrum of compound **3**^ (DMSO-*d*6, 500 MHz)

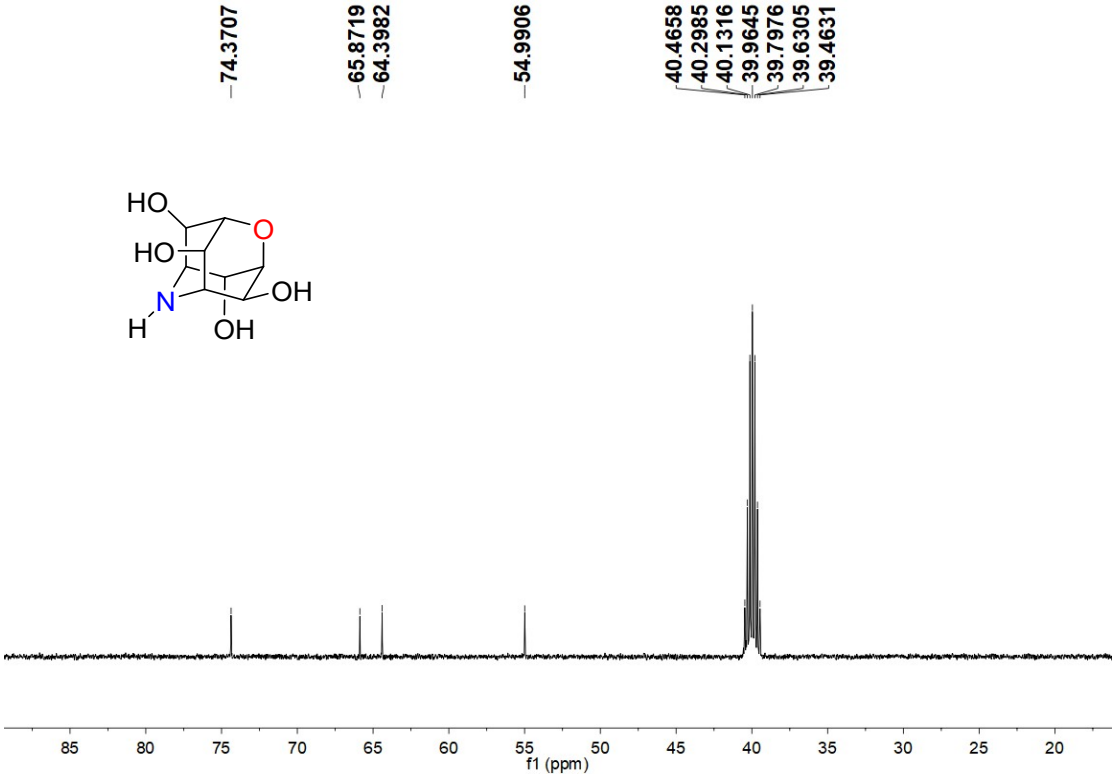

Fig.S15 ^{13}C NMR spectrum of compound **11** (DMSO-*d*6, 126 MHz)

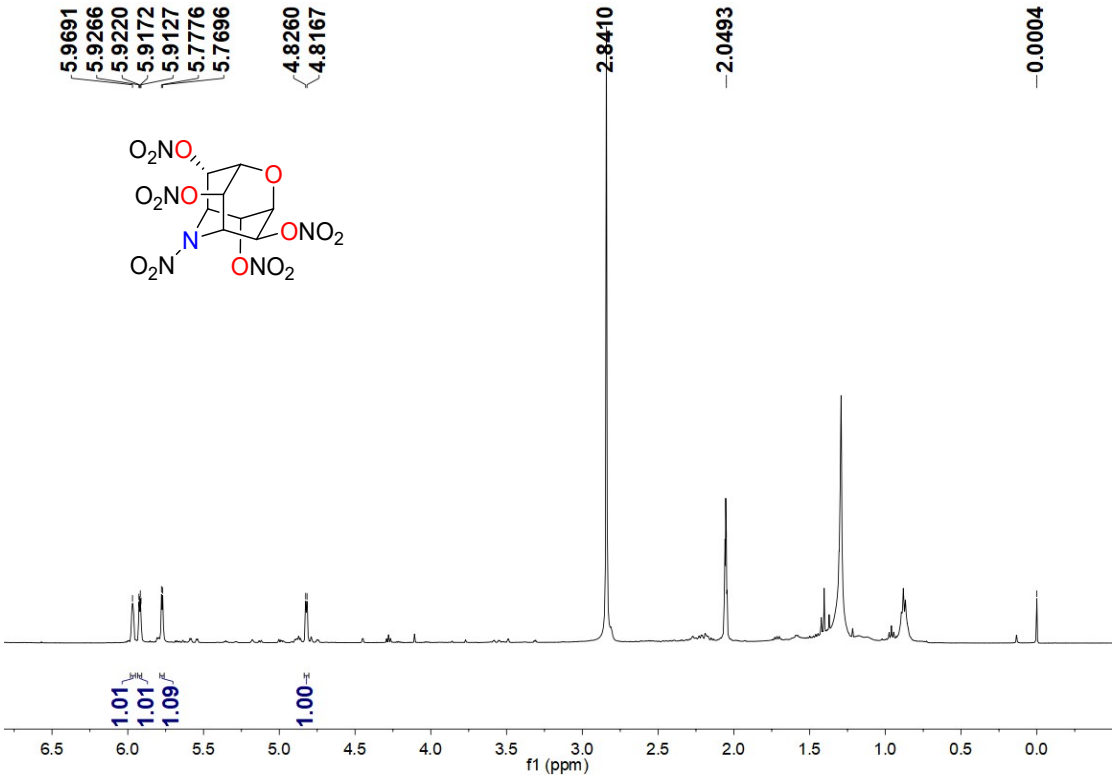

Fig.S16 ^{1}H NMR spectrum of compound **3** (acetone-*d*6, 500 MHz)

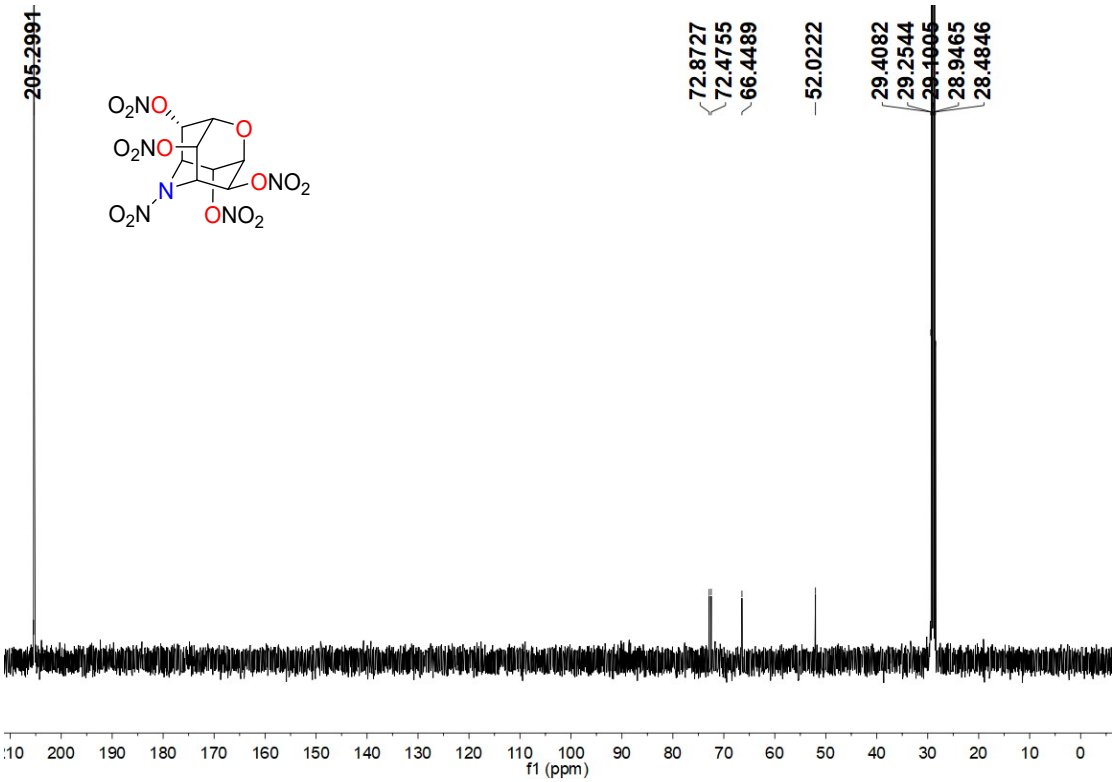

Fig.S17 ^{13}C NMR spectrum of compound **3** (acetone-*d*6, 126 MHz)

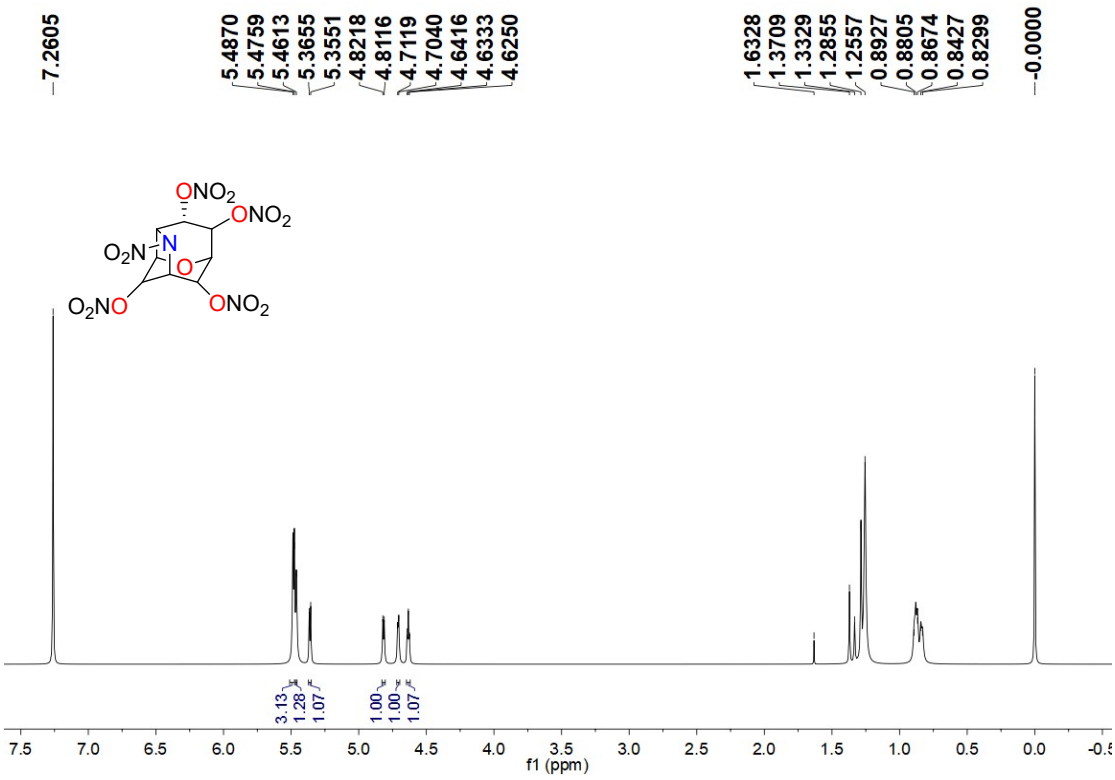

Fig.S18 ^{1}H NMR spectrum of compound **4** ($CDCl_3$, 500 MHz)

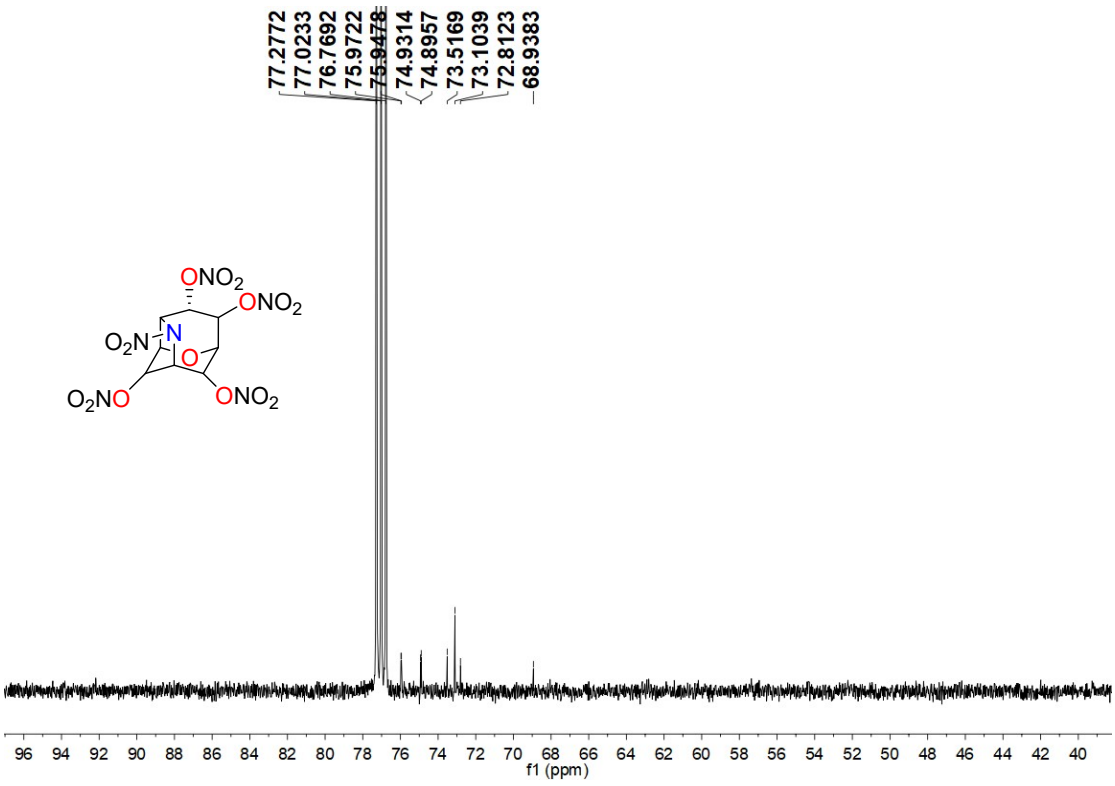

Fig.S19 ^{13}C NMR spectrum of compound **4** ($CDCl_3$, 126 MHz)

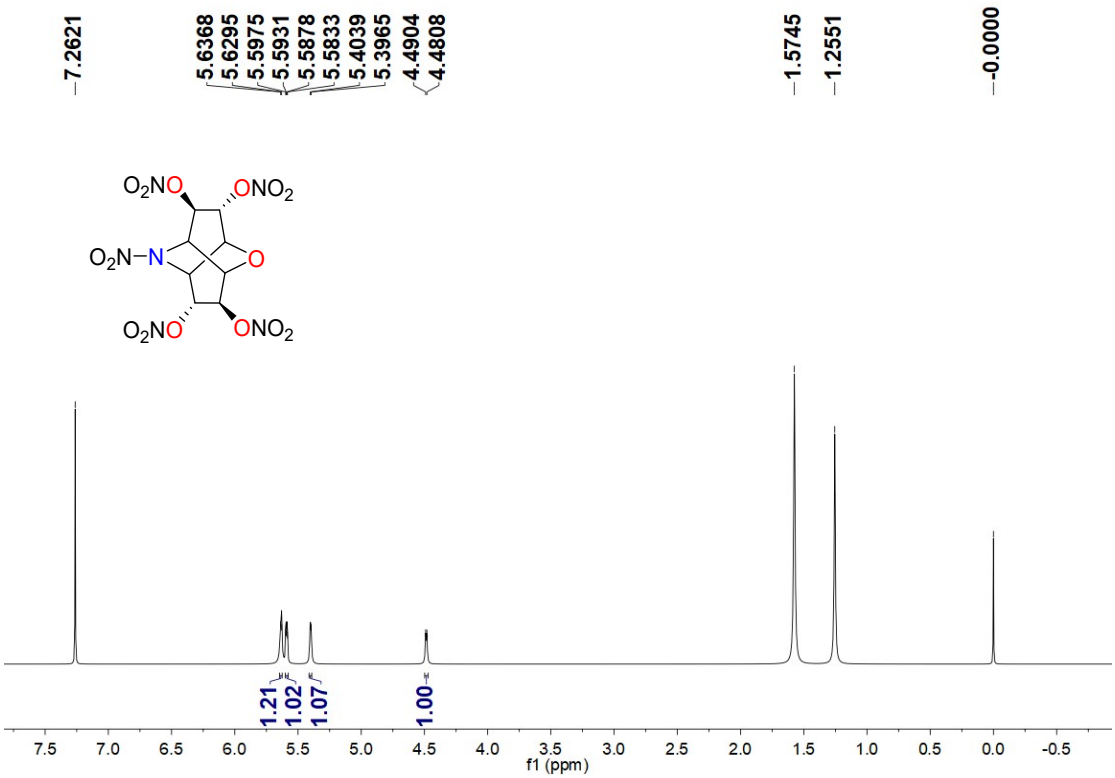

Fig.S20 ^{1}H NMR spectrum of compound **5** ($CDCl_3$, 500 MHz)

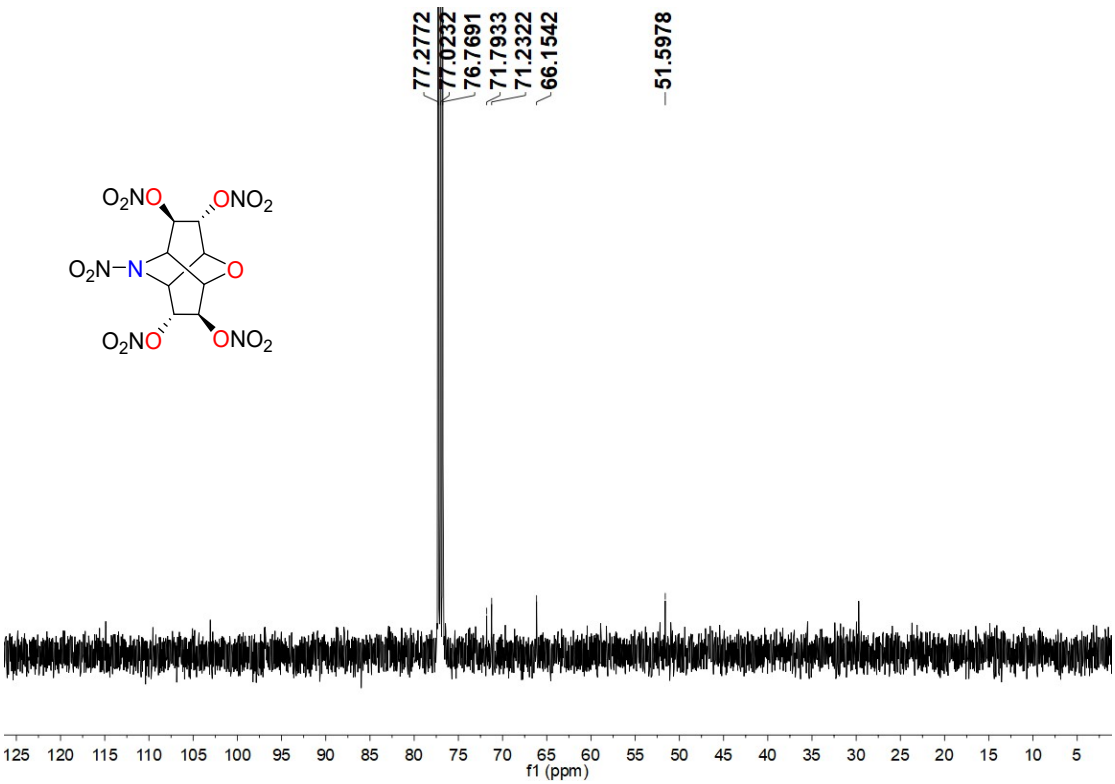

Fig.S21 ^{13}C NMR spectrum of compound **5** ($CDCl_3$, 126 MHz)

5. IR spectra of Compounds

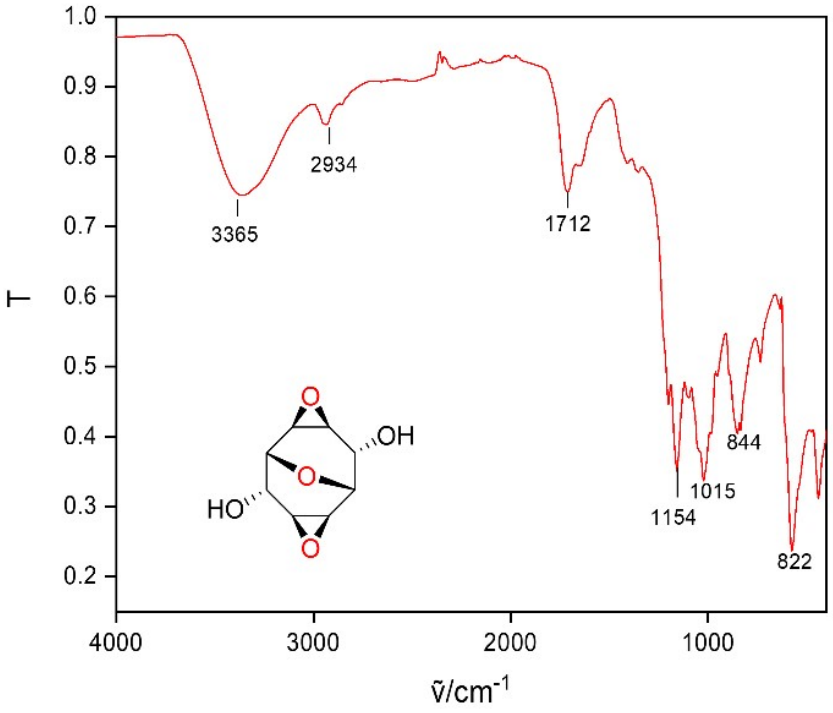

Fig.S22 IR spectrum of **10**.

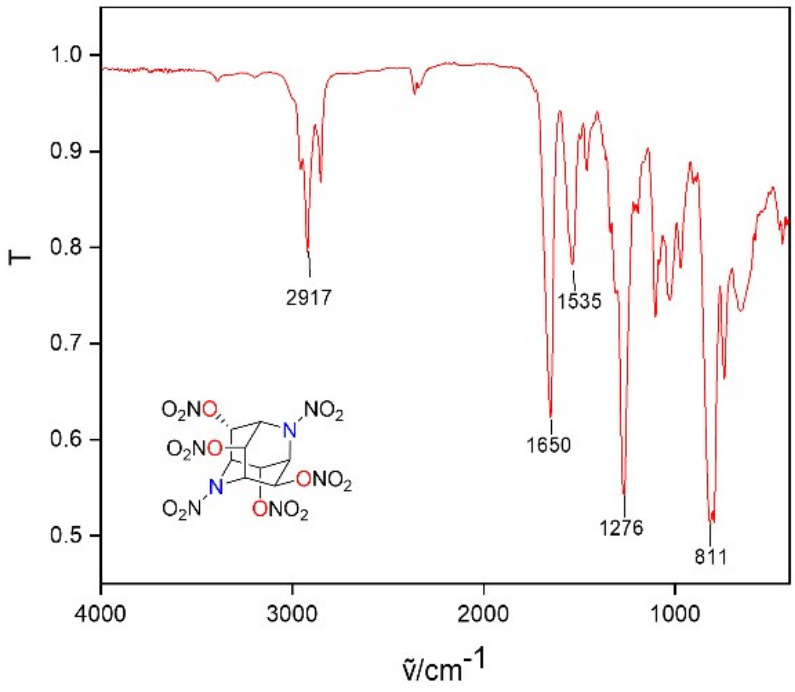

Fig.S23 IR spectrum of **1**.

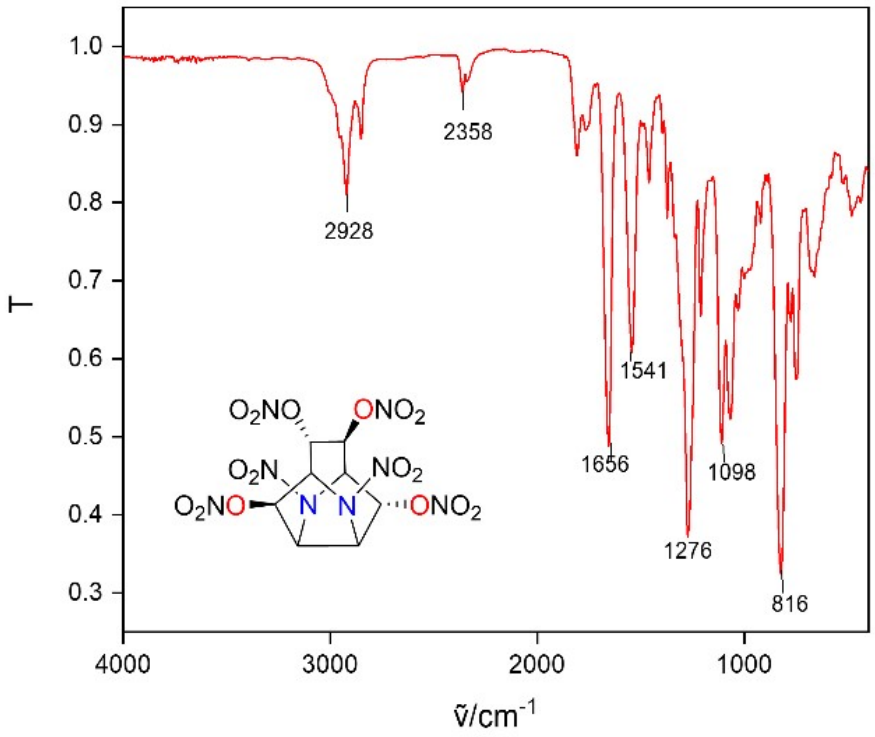

Fig.S24 IR spectrum of **2**.

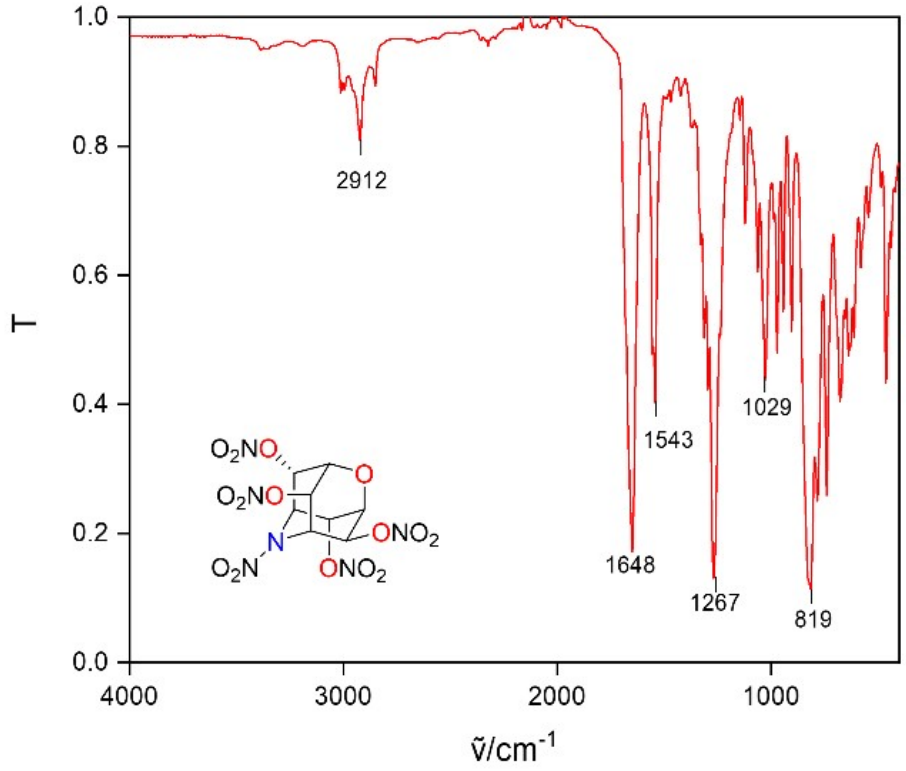

Fig.S25 IR spectrum of **3**.

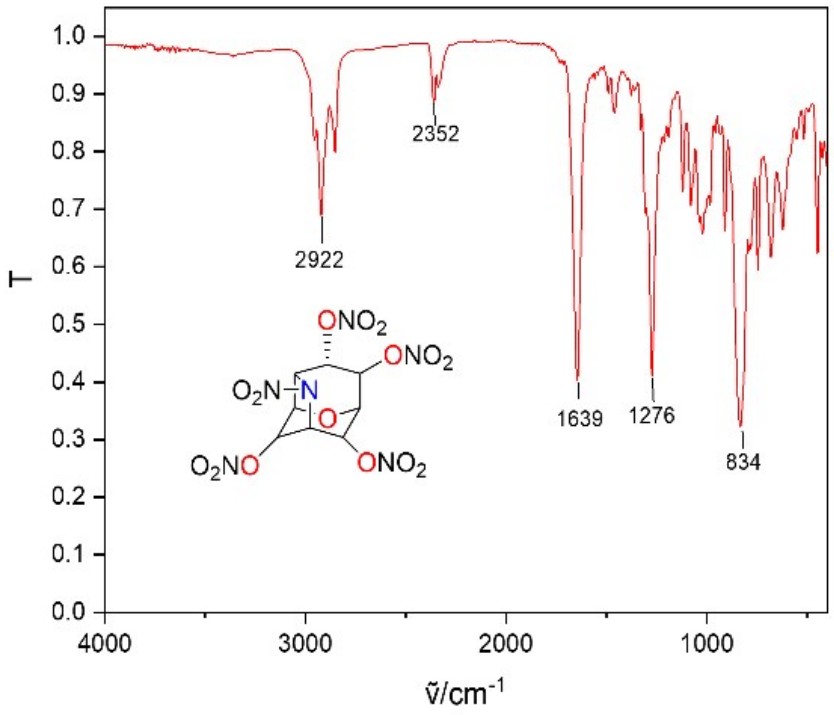

Fig.S26 IR spectrum of **4**.

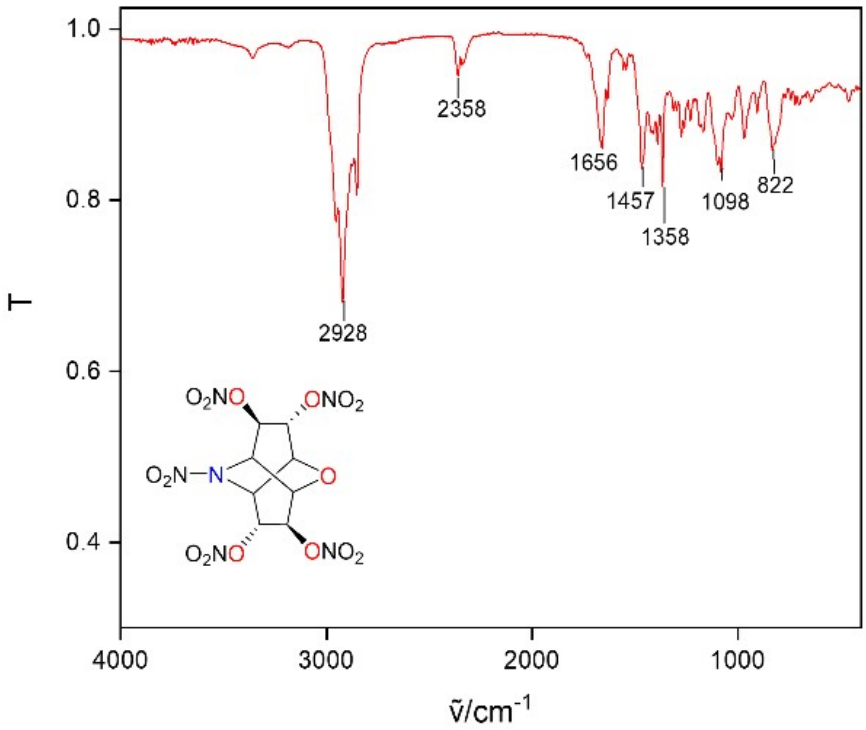

Fig.S27 IR spectrum of **5**.

6. TG-DSC curves

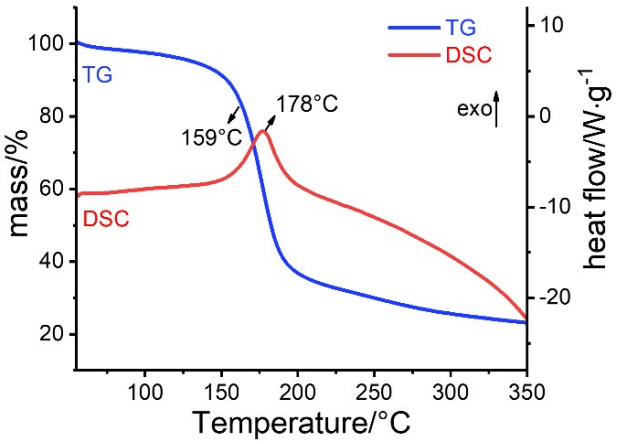

Fig.S28 TG-DSC curves of **1**

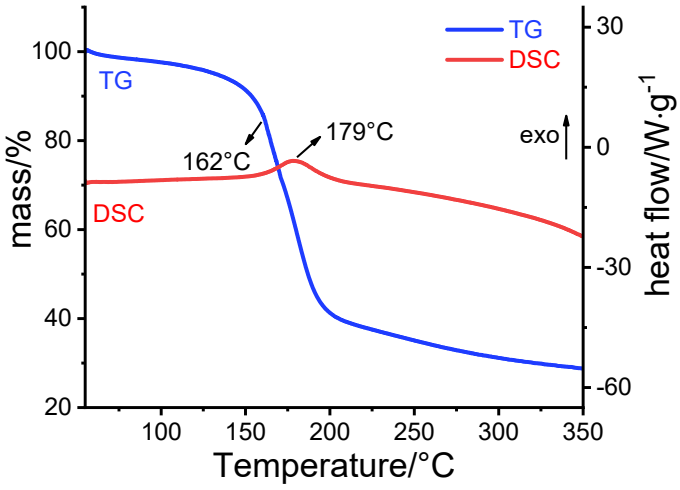

Fig.S29 TG-DSC curves of **2**

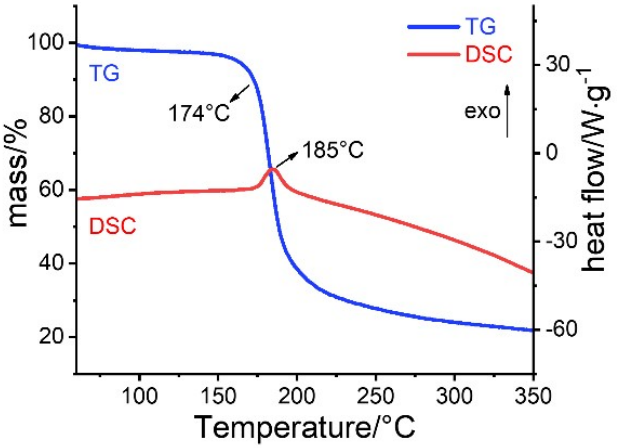

Fig.S30 TG-DSC curves of **3**

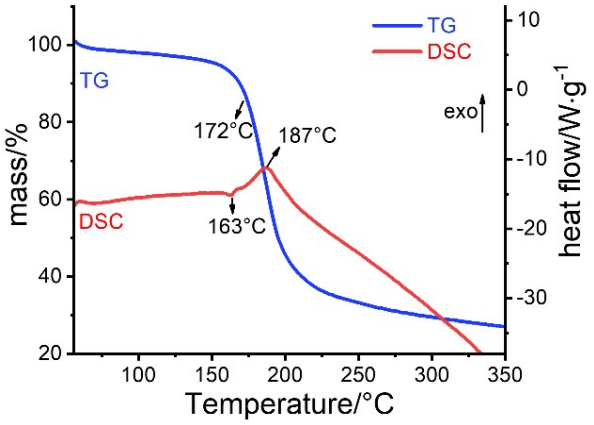

Fig.S31 TG-DSC curves of **4**

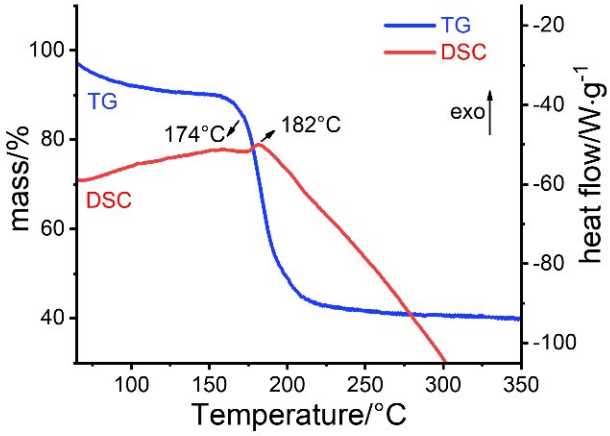

Fig.S32 TG-DSC curves of **5**

7. ESP-mapped vdW surfaces

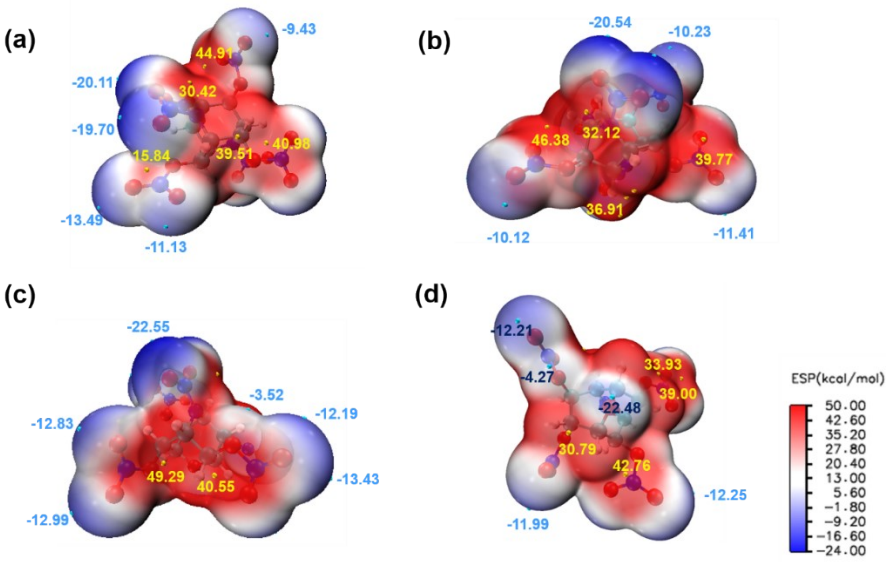

Fig.S33 ESP-mapped vdW surfaces of compound **1** (a), **2** (b) , **3** (c) , **4** (d).

8. References

1. G. Wang, X. Gong, H. Du, Y. Liu and H. Xiao, Theoretical Prediction of Properties of Aliphatic Polynitrates, *The Journal of Physical Chemistry A*, 2011, **115**(5), 795-804.
2. G. Wang, X. Gong, Y. Liu, H. Du, X. Xu, and H. Xiao, Looking for high energy density compounds applicable for propellant among the derivatives of DPO with $-N_3$, $-ONO_2$, and $-NNO_2$ groups, *Journal of Computational Chemistry*, 2011, **32**(5), 943-952.
3. Y. Xu, G. Wang, Y. Liu, P. Gao, and X. Gong, Theoretical investigations on the density, detonation performance and stability of fluorinated hexanitroadamantanes, *Structural Chemistry*, 2021, **32**, 1651-1657.
4. L. Qiu, H. Xiao, X. Gong, X. Ju, and W. Zhu, Crystal density predictions for nitramines based on quantum chemistry, *Journal of Hazardous Materials*, 2007, **141**(1), 280-288.
5. G. Wang, X. Gong, Y. Liu, H. Du and H. Xiao, Prediction of crystalline densities of polynitro arenes for estimation of their detonation performance based on quantum chemistry, *Journal of Molecular Structure: THEOCHEM*, 2010, **953**(1-3), 163-169.